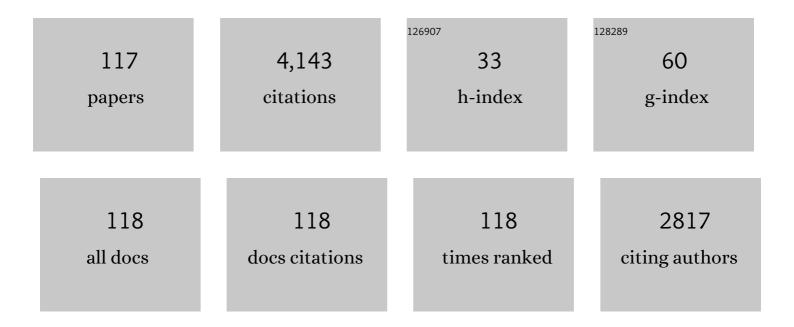
List of Publications by Year in descending order

Source: https://exaly.com/author-pdf/3203826/publications.pdf Version: 2024-02-01



#	Article	IF	CITATIONS
1	Highly Improved Microwave Absorbing and Mechanical Properties in Cold Sintered ZnO by Incorporating Graphene Oxide. Journal of the European Ceramic Society, 2022, 42, 993-1000.	5.7	31
2	Hardness and toughness improvement of SiCâ€based ceramics with the addition of (Hf <sub>0.2</sub> Mo <sub>0.2</sub> Ta <sub>0.2</sub> Nb <sub>0.2</sub> Ti <sub>0.2</sub> B <sub>2</sub> . Journal of the American Ceramic Society, 2022, 105, 1629-1634.	3.8	7
3	Significantly reduced conductivity in strontium titanate-based lead-free ceramics by excess bismuth. Materials Letters, 2022, 309, 131453.	2.6	8
4	Ceramic-based stabilization/solidification of radioactive waste. , 2022, , 449-468.		1
5	Lattice occupying sites and microwave dielectric properties of Mg2+–Si4+ co-doped MgxY3-xAl5-xSixO12 garnet typed ceramics. Journal of Materials Science: Materials in Electronics, 2022, 33, 2116-2124.	2.2	12
6	Design of a Sub-6 GHz Dielectric Resonator Antenna with Novel Temperature-Stabilized (Sm <sub>1–<i>x</i></sub> Bi <sub><i>x</i></sub> )NbO <sub>4</sub> ( <i>x</i> = 0–0.15) Microwave Dielectric Ceramics. ACS Applied Materials & Interfaces, 2022, 14, 7030-7038.	8.0	52
7	Temperature-dependent discharge performance of (Pb0.87Ba0.08Sr0.02La0.02) (Zr0.65Sn0.27Ti0.08) O3 antiferroelectric ceramics. Journal of Materials Science: Materials in Electronics, 2022, 33, 5468.	2.2	1
8	Ultra-low temperature co-fired ceramics with adjustable microwave dielectric properties in the Na <sub>2</sub> O–Bi <sub>2</sub> O <sub>3</sub> –MoO <sub>3</sub> ternary system: a comprehensive study. Journal of Materials Chemistry C, 2022, 10, 2008-2016.	5.5	65
9	Perspectives on Working Voltage of Aqueous Supercapacitors. Small, 2022, 18, e2106360.	10.0	93
10	Low permittivity cordierite-based microwave dielectric ceramics for 5G/6G telecommunications. Journal of the European Ceramic Society, 2022, 42, 2820-2826.	5.7	76
11	Chemical characterisation of degraded nuclear fuel analogues simulating the Fukushima Daiichi nuclear accident. Npj Materials Degradation, 2022, 6, .	5.8	3
12	Microwave dielectric properties of Mg1.8R0.2Al4Si5O18 (R = Mg, Ca, Sr, Ba, Mn, Co, Ni, Cu, Zn) cordierite ceramics and their application for 5G microstrip patch antenna. Journal of the European Ceramic Society, 2022, 42, 2254-2260.	5.7	33
13	Sn4+ induced Bi3+ multi-lattice selective occupation and its color-tunable emission of La2MgZrO6: Bi3+, Sn4+ double perovskite phosphors. Journal of Alloys and Compounds, 2022, 902, 163724.	5.5	15
14	Crystal structure and microwave dielectric properties of Mg2+-Si4+ co-modified yttrium aluminum garnet ceramics. Journal of Materials Science: Materials in Electronics, 2022, 33, 4712-4720.	2.2	11
15	Synthesis and characterisation of Ce-doped zirconolite Ca0.80Ce0.20ZrTi1.60M0.40O7 (M = Fe, Al) formed by reactive spark plasma sintering (RSPS). MRS Advances, 2022, 7, 75-80.	0.9	8
16	Remarkably enhanced photocatalytic performance of Au/AgNbO3 heterostructures by coupling piezotronic with plasmonic effects. Nano Energy, 2022, 95, 107031.	16.0	51
17	Dense SiC ceramics prepared by using amorphous sintering additives. Ceramics International, 2022, 48, 16449-16454.	4.8	5
18	Dielectric temperature stability and energy storage performance of NBTâ€based ceramics by introducing highâ€entropy oxide. Journal of the American Ceramic Society, 2022, 105, 4796-4804.	3.8	73

#	Article	IF	CITATIONS
19	Phase Evolution in the CaZrTi <sub>2</sub> O <sub>7</sub> –Dy <sub>2</sub> Ti <sub>2</sub> O <sub>7</sub> System: A Potential Host Phase for Minor Actinide Immobilization. Inorganic Chemistry, 2022, 61, 5744-5756.	4.0	12
20	Effect of native carbon vacancies on evolution of defects in ZrC1- under He ion irradiation and annealing. Journal of Materials Science and Technology, 2022, 119, 87-97.	10.7	5
21	Bottom-up synthesis of 2D layered high-entropy transition metal hydroxides. Nanoscale Advances, 2022, 4, 2468-2478.	4.6	17
22	Highâ€Temperature Flexible Nanocomposites with Ultraâ€High Energy Storage Density by Nanostructured MgO Fillers. Advanced Functional Materials, 2022, 32, .	14.9	41
23	Lead-free borosilicate glass/fused quartz composites for LTCC applications. Journal of Materials Science: Materials in Electronics, 2022, 33, 15033-15038.	2.2	8
24	High Q×f values of Zn-Ni co-modified LiMg0.9Zn0.1-Ni PO4 microwave dielectric ceramics for 5G/6G LTCC modules. Journal of the European Ceramic Society, 2022, 42, 5684-5690.	5.7	34
25	Properties and microstructure of basic magnesium sulfate cement: Influence of silica fume. Construction and Building Materials, 2021, 266, 121076.	7.2	33
26	Mechanism of enhanced energy storage density in AgNbO3-based lead-free antiferroelectrics. Nano Energy, 2021, 79, 105423.	16.0	180
27	Effects of the joining process on the microstructure and properties of liquid-phase-sintered SiC-SiC joints formed with Ti foil. Journal of the European Ceramic Society, 2021, 41, 225-232.	5.7	11
28	Fabrication of textured (Hf0.2Zr0.2Ta0.2Cr0.2Ti0.2)B2 high-entropy ceramics. Journal of the European Ceramic Society, 2021, 41, 1015-1019.	5.7	40
29	Characterization of and Structural Insight into Struvite-K, MgKPO <sub>4</sub> ·6H <sub>2</sub> O, an Analogue of Struvite. Inorganic Chemistry, 2021, 60, 195-205.	4.0	29
30	Synthesis, structure, and characterization of the thorium zirconolite CaZr <sub>1â€x</sub> Th <sub>x</sub> Ti <sub>2</sub> O <sub>7</sub> system. Journal of the American Ceramic Society, 2021, 104, 2937-2951.	3.8	12
31	On the existence of the compound "Ce3NbO7+―prepared under air atmosphere. Journal of Rare Earths, 2021, 39, 596-599.	4.8	4
32	Optimal preparation of high-entropy boride-silicon carbide ceramics. Journal of Advanced Ceramics, 2021, 10, 173-180.	17.4	52
33	Synthesis of zirconolite-2M ceramics for immobilisation of neptunium. Ceramics International, 2021, 47, 1047-1052.	4.8	1
34	Safely probing the chemistry of Chernobyl nuclear fuel using micro-focus X-ray analysis. Journal of Materials Chemistry A, 2021, 9, 12612-12622.	10.3	8
35	Temperature stable Sm(Nb <sub>1â^'x</sub> V <sub>x</sub> )O <sub>4</sub> (0.0 ≤i>x ≤0.9) microwave dielectric ceramics with ultra-low dielectric loss for dielectric resonator antenna applications. Journal of Materials Chemistry C, 2021, 9, 9962-9971.	5.5	60
36	Review of zirconolite crystal chemistry and aqueous durability. Advances in Applied Ceramics, 2021, 120, 69-83.	1.1	25

#	Article	IF	CITATIONS
37	Dense and coreâ€rim structured B 4 Câ€TiB 2 ceramics with Moâ€Coâ€WC additive. Journal of the American Ceramic Society, 2021, 104, 2860-2867.	3.8	7
38	New lowâ€ <i>ε<sub>r</sub></i> , temperature stable Mg <sub>3</sub> B <sub>2</sub> O <sub>6</sub> â€Ba <sub>3</sub> (VO <sub>4</sub> ) <sub>2</sub> microwave composite ceramic for 5G application. Journal of the American Ceramic Society, 2021, 104, 3818-3822.	3.8	25
39	Synthesis and characterisation of HIP Ca0.80Ce0.20ZrTi1.60Cr0.40O7 zirconolite and observations of the ceramic–canister interface. MRS Advances, 2021, 6, 112-118.	0.9	3
40	Low-temperature catalytic combustion of benzene over Zr–Mn mixed oxides synthesized by redox-precipitation method. Journal of Materials Science, 2021, 56, 13540-13555.	3.7	6
41	Core-Shell Structure and Dielectric Properties of Ba0.6Sr0.4TiO3@ Fe2O3 Ceramics Prepared by Co-Precipitation Method. Crystals, 2021, 11, 623.	2.2	4
42	Influence of accessory phases and surrogate type on accelerated leaching of zirconolite wasteforms. Npj Materials Degradation, 2021, 5, .	5.8	8
43	Ultrahigh energy density in short-range tilted NBT-based lead-free multilayer ceramic capacitors by nanodomain percolation. Energy Storage Materials, 2021, 38, 113-120.	18.0	139
44	Temperature Stable, High-Quality Factor Li2TiO3-Li4NbO4F Microwave Dielectric Ceramics. Crystals, 2021, 11, 741.	2.2	5
45	Powder synthesis, densification, microstructure and mechanical properties of Hf-based ternary boride ceramics. Journal of the European Ceramic Society, 2021, 41, 3922-3928.	5.7	13
46	Efficient toluene adsorption/desorption on biochar derived from in situ acid-treated sugarcane bagasse. Environmental Science and Pollution Research, 2021, 28, 62616-62627.	5.3	9
47	5G microstrip patch antenna and microwave dielectric properties of cold sintered LiWVO6–K2MoO4 composite ceramics. Ceramics International, 2021, 47, 19241-19246.	4.8	37
48	High-entropy A2B2O7-type oxide ceramics: A potential immobilising matrix for high-level radioactive waste. Journal of Hazardous Materials, 2021, 415, 125596.	12.4	59
49	High-Quality-Factor AlON Transparent Ceramics for 5 GHz Wi-Fi Aesthetically Decorative Antennas. ACS Applied Materials & Interfaces, 2021, 13, 46866-46874.	8.0	16
50	Chemical state mapping of simulant Chernobyl lava-like fuel containing material using micro-focused synchrotron X-ray spectroscopy. Journal of Synchrotron Radiation, 2021, 28, 1672-1683.	2.4	4
51	Synergy of nanodiamond–doxorubicin conjugates and PD-L1 blockade effectively turns tumor-associated macrophages against tumor cells. Journal of Nanobiotechnology, 2021, 19, 268.	9.1	25
52	Conjugation with nanodiamonds via hydrazone bond fundamentally alters intracellular distribution and activity of doxorubicin. International Journal of Pharmaceutics, 2021, 606, 120872.	5.2	10
53	Lattices selective occupation, optical spectra regulation, and photoluminescence properties of Eu2+ activated Ca9La(PO4)7 phosphor. Journal of Luminescence, 2021, 237, 118197.	3.1	9
54	Nanoplates forced alignment of multi-walled carbon nanotubes in alumina composite with high strength and toughness. Journal of the European Ceramic Society, 2021, 41, 5541-5547.	5.7	9

#	Article	IF	CITATIONS
55	Influence of TiB2 and CrB2 on densification, microstructure, and mechanical properties of ZrB2 ceramics. Ceramics International, 2021, 47, 28008-28013.	4.8	8
56	Synthesis of Ca1-xCexZrTi2-2xAl2xO7 zirconolite ceramics for plutonium disposition. Journal of Nuclear Materials, 2021, 556, 153198.	2.7	8
57	Engineering lithiophilic Ni-Al@LDH interlayers on a garnet-type electrolyte for solid-state lithium metal batteries. Chemical Communications, 2021, 57, 10214-10217.	4.1	7
58	Low-Temperature Nitridation of Fe <sub>3</sub> O <sub>4</sub> by Reaction with NaNH <sub>2</sub> . Inorganic Chemistry, 2021, 60, 2553-2562.	4.0	3
59	Synthesis of single-phase metal oxycarbonitride ceramics. Scripta Materialia, 2020, 176, 17-22.	5.2	18
60	Improvement of densification and microstructure of HfB <sub>2</sub> ceramics by Ta/Ti substitution for Hf. Journal of the American Ceramic Society, 2020, 103, 103-111.	3.8	16
61	A new approach to the immobilisation of technetium and transuranics: Co-disposal in a zirconolite ceramic matrix. Journal of Nuclear Materials, 2020, 528, 151885.	2.7	9
62	Lowâ€ŧemperature joining of SiC ceramics using NITE phase with Al 2 O 3 â€Ho 2 O 3 additive. Journal of the American Ceramic Society, 2020, 103, 731-736.	3.8	10
63	Lead-free (Ba,Sr)TiO3 – BiFeO3 based multilayer ceramic capacitors with high energy density. Journal of the European Ceramic Society, 2020, 40, 1779-1783.	5.7	79
64	Rapid synthesis of zirconolite ceramic wasteform by microwave sintering for disposition of plutonium. Journal of Nuclear Materials, 2020, 539, 152332.	2.7	6
65	Novel BaTiO <sub>3</sub> -Based, Ag/Pd-Compatible Lead-Free Relaxors with Superior Energy Storage Performance. ACS Applied Materials & Interfaces, 2020, 12, 43942-43949.	8.0	130
66	Crystal and Electronic Structures of A <sub>2</sub> NaIO <sub>6</sub> Periodate Double Perovskites (A = Sr, Ca, Ba): Candidate Wasteforms for I-129 Immobilization. Inorganic Chemistry, 2020, 59, 18407-18419.	4.0	13
67	Synthesis and characterisation of Ca1-xCexZrTi2-2xCr2xO7: Analogue zirconolite wasteform for the immobilisation of stockpiled UK plutonium. Journal of the European Ceramic Society, 2020, 40, 5909-5919.	5.7	29
68	Fatigue resistant lead-free multilayer ceramic capacitors with ultrahigh energy density. Journal of Materials Chemistry A, 2020, 8, 11414-11423.	10.3	114
69	Cold sintered LiMgPO <sub>4</sub> based composites for low temperature coâ€fired ceramic (LTCC) applications. Journal of the American Ceramic Society, 2020, 103, 6237-6244.	3.8	45
70	Improved densification and hardness of high-entropy diboride ceramics from fine powders synthesized via borothermal reduction process. Ceramics International, 2020, 46, 14299-14303.	4.8	49
71	Pressureless joining of silicon carbide using Ti3SiC2 MAX phase at 1500oC. Ceramics International, 2020, 46, 14269-14272.	4.8	15
72	A systematic investigation of the phase assemblage and microstructure of the zirconolite CaZr1-xCexTi2O7 system. Journal of Nuclear Materials, 2020, 535, 152137.	2.7	26

SHI-KUAN SUN

#	Article	IF	CITATIONS
73	Direct Integration of Cold Sintered, Temperature-Stable Bi2Mo2O9-K2MoO4 Ceramics on Printed Circuit Boards for Satellite Navigation Antennas. Journal of the European Ceramic Society, 2020, 40, 4029-4034.	5.7	52
74	Improvement of sinterability and mechanical properties of ZrB2 ceramics by the modified borothermal reduction methods. Journal of the European Ceramic Society, 2020, 40, 3844-3850.	5.7	7
75	Reactive spark plasma sintering of Cs-exchanged chabazite: characterisation and durability assessment for Fukushima Daiichi NPP clean-up. Journal of Nuclear Science and Technology, 2019, 56, 891-901.	1.3	15
76	Dense and pure high-entropy metal diboride ceramics sintered from self-synthesized powders via boro/carbothermal reduction approach. Science China Materials, 2019, 62, 1898-1909.	6.3	89
77	Continuous and symmetric graded Si3N4 ceramics designed by spark plasma sintering at 15†MPa. Ceramics International, 2019, 45, 16703-16706.	4.8	16
78	Nano-infiltration and transient eutectic (NITE) phase joining SiC ceramics at 1500oC. Ceramics International, 2019, 45, 24927-24931.	4.8	24
79	Low-temperature joining of silicon carbide via Al-air in situ reaction. Ceramics International, 2019, 45, 24932-24935.	4.8	1
80	Preparation and oxidation behaviour of SiC-based ceramics with TaB2 addition. Ceramics International, 2019, 45, 23836-23840.	4.8	9
81	Microstructure evolution of MeB2 (Me=Zr, Ti) powders prepared by borothermal reduction during heat treatment at 1000°C–1800°C. Ceramics International, 2019, 45, 23794-23797.	4.8	2
82	Selection principle of the synthetic route for fabrication of HfB <sub>2</sub> and HfB <sub>2</sub> â€ <b>s</b> iC ceramics. Journal of the American Ceramic Society, 2019, 102, 6427-6432.	3.8	13
83	Microstructure and mechanical properties of high-entropy borides derived from boro/carbothermal reduction. Journal of the European Ceramic Society, 2019, 39, 3920-3924.	5.7	127
84	High-temperature stability and densification of Ti-substituted ZrB2-based ceramics. Ceramics International, 2019, 45, 15749-15753.	4.8	12
85	Dense high-entropy boride ceramics with ultra-high hardness. Scripta Materialia, 2019, 164, 135-139.	5.2	177
86	Powder characteristics, sinterability, and mechanical properties of TiB <sub>2</sub> prepared by three reduction methods. Journal of the American Ceramic Society, 2019, 102, 4511-4519.	3.8	12
87	Pressureless joining of SiC ceramics at low temperature. Ceramics International, 2019, 45, 6556-6559.	4.8	11
88	Direct synthesis of nearly single phase SrTaO2N from SrCO3/TaN. Ceramics International, 2018, 44, 4504-4507.	4.8	7
89	Effect of CeO <sub>2</sub> and Al <sub>2</sub> O <sub>3</sub> contents on Ceâ€ZrO <sub>2</sub> /Al <sub>2</sub> O <sub>3</sub> composites. Journal of the American Ceramic Society, 2018, 101, 2066-2073.	3.8	5
90	Reactive spark plasma synthesis of CaZrTi2O7 zirconolite ceramics for plutonium disposition. Journal of Nuclear Materials, 2018, 500, 11-14.	2.7	27

#	Article	IF	CITATIONS
91	BiFeO <sub>3</sub> -BaTiO <sub>3</sub> : A new generation of lead-free electroceramics. Journal of Advanced Dielectrics, 2018, 08, 1830004.	2.4	166
92	Synthesis of perovskite BaTaO2N and SrNbO2N using TaN/NbN as the nitrogen source. Ceramics International, 2018, 44, 23324-23328.	4.8	8
93	High Energy Storage Density and Large Strain in Bi(Zn <sub>2/3</sub> Nb <sub>1/3</sub> )O <sub>3</sub> -Doped BiFeO <sub>3</sub> –BaTiO <sub>3</sub> Ceramics. ACS Applied Energy Materials, 2018, 1, 4403-4412.	5.1	229
94	Structural evolution in ZrC-SiC composite irradiated by 4†MeV Au ions. Nuclear Instruments & Methods in Physics Research B, 2018, 434, 23-28.	1.4	18
95	Effect of ZrB <sub>2</sub> content on phase assemblage and mechanical properties of Si <sub>3</sub> N <sub>4</sub> –ZrB <sub>2</sub> ceramics prepared at low temperature. Journal of the American Ceramic Society, 2018, 101, 4870-4875.	3.8	13
96	Structure analysis of vitusite glass–ceramic waste forms using extended X-ray absorption fine structures. Ceramics International, 2017, 43, 4687-4691.	4.8	5
97	Texture, microstructures, and mechanical properties of AlNâ€based ceramics with Si <sub>3</sub> N <sub>4</sub> –Y <sub>2</sub> O <sub>3</sub> additives. Journal of the American Ceramic Society, 2017, 100, 3380-3384.	3.8	23
98	Graded Si3N4 ceramics with hard surface and tough core by two-step hot pressing. Ceramics International, 2017, 43, 7948-7950.	4.8	10
99	Particle refinement of ZrB <sub>2</sub> by the combination of borothermal reduction and solid solution. Journal of the American Ceramic Society, 2017, 100, 524-528.	3.8	13
100	Additive sintering and post-ammonolysis of dielectric BaTaO2N oxynitride perovskite. Journal of the European Ceramic Society, 2016, 36, 3341-3345.	5.7	25
101	Ferroelectric Response Induced in <i>cis</i> -Type Anion Ordered SrTaO <sub>2</sub> N Oxynitride Perovskite. Chemistry of Materials, 2016, 28, 1312-1317.	6.7	61
102	Processing of dielectric oxynitride perovskites for powders, ceramics, compacts and thin films. Dalton Transactions, 2015, 44, 10570-10581.	3.3	42
103	Direct synthesis of nearly single-phase BaTaO2N and CaTaO2N powders. Journal of the European Ceramic Society, 2015, 35, 3289-3294.	5.7	15
104	Preparation and luminescence properties of Eu2+-doped oxynitride feldspar SrAl2â^'Si2+O8â^'N. Journal of Alloys and Compounds, 2015, 618, 254-257.	5.5	4
105	Additive Sintering, Postannealing, and Dielectric Properties of <scp><scp>SrTaO</scp></scp> <sub>2</sub> <scp><scp>N</scp>. Journal of the American Ceramic Society, 2014, 97, 1023-1027.</scp>	3.8	45
106	Reactive spark plasma sintering of binderless WC ceramics at 1500°C. International Journal of Refractory Metals and Hard Materials, 2014, 43, 42-45.	3.8	27
107	Direct synthesis of SrTaO2N from SrCO3/Ta3N5 involving CO evolution. Journal of the European Ceramic Society, 2014, 34, 4451-4455.	5.7	22
108	Reactive spark plasma sintering of ZrC and HfC ceramics with fine microstructures. Scripta Materialia, 2013, 69, 139-142.	5.2	59

#	Article	IF	CITATIONS
109	Reaction Sintering of <scp><scp>HfC</scp></scp> / <scp>W</scp> Cermets with High Strength and Toughness. Journal of the American Ceramic Society, 2013, 96, 867-872.	3.8	19
110	Synthesis mechanism and sintering behavior of tungsten carbide powder produced by a novel solid state reaction of W2N. International Journal of Refractory Metals and Hard Materials, 2012, 35, 202-206.	3.8	13
111	Structure-property relationships in manganese oxide - mesoporous silica nanoparticles used for T1-weighted MRI and simultaneous anti-cancer drug delivery. Biomaterials, 2012, 33, 2388-2398.	11.4	135
112	Chemical Reactions, Anisotropic Grain Growth and Sintering Mechanisms of Self-Reinforced ZrB2-SiC Doped with WC. Journal of the American Ceramic Society, 2011, 94, 1575-1583.	3.8	91
113	Fabrication of Nanosized Tungsten Carbide Ceramics by Reactive Spark Plasma Sintering. Journal of the American Ceramic Society, 2011, 94, 3230-3233.	3.8	20
114	A microexplosion method for the synthesis of graphene nanoribbons. Carbon, 2011, 49, 1439-1445.	10.3	12
115	ZrO2 removing reactions of Groups IV–VI transition metal carbides in ZrB2 based composites. Journal of the European Ceramic Society, 2011, 31, 421-427.	5.7	45
116	Preparation and electrical properties of graphene nanosheet/Al2O3 composites. Carbon, 2010, 48, 1743-1749.	10.3	315
117	Ultraâ€Fine Tungsten Carbide Powder Prepared by a Nitridation–Carburization Method. Journal of the American Ceramic Society, 2010, 93, 3565-3568.	3.8	11